Defect characterization studies on highly irradiated Low Gain Avalanche Detectors

EP-DT-DD
Detector Technologies
Detector Development

Anja Himmerlich, Nuria Castello-Mor, Esteban Curras Rivera,
Yana Gurimskaya, Vendula Maulerova-Subert, Michael Moll
CERN, Switzerland

Ioana Pintilie
NIMP, Bucharest-Magurele, Romania

Universität Hamburg
DER FORSCHUNG | DER LEHRE | DER BILDUNG

Chuan Liao, Eckhart Fretwurst, Joern Schwandt
University Hamburg, Germany

BELARUSIAN STATE UNIVERSITY

Leonid Makarenko
Belarusian State University, Minsk, Belarus

Motivation

Moll, PoS 2019 VERTEX

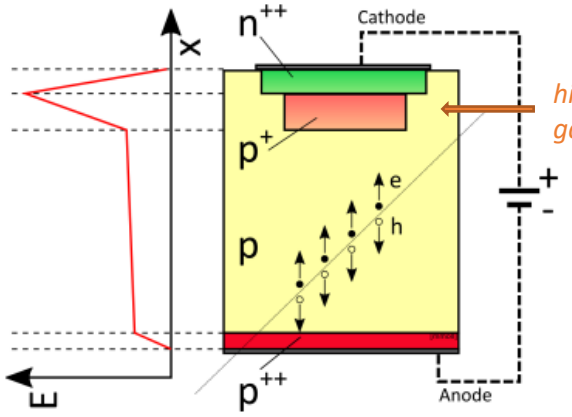

highly boron-doped gain-layer (1E+17 cm-3)

High energy particles (n, p^+, e^- …) → ***Si (LGAD)*** → E_K>25 eV → Vacancy + Interstitial → *point defects (V-O, C-O, ..)*

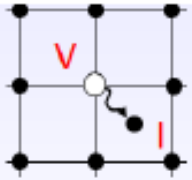

Si (LGAD) → $E_K > 5$ keV → *point defects and clusters of defects*

⟹ *radiation induced degradation of the highly boron-doped gain-layer*

⟹ *decrease of the signal gain with increasing particle fluence*

*„boron deactivation“ ⟹ ACCEPTOR REMOVAL EFFECT by **BiOi** formation*

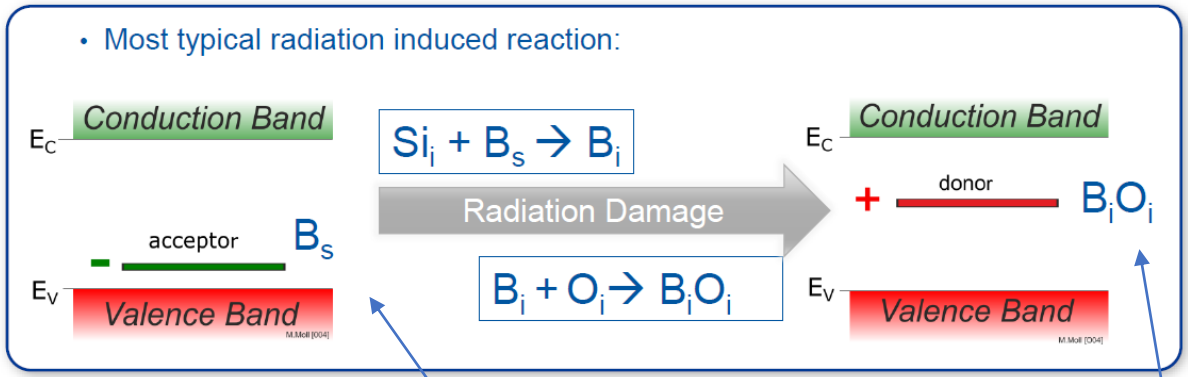

*induce **negative** space charge*

*induce **positive** space charge*

Motivation

Moll, PoS 2019 VERTEX

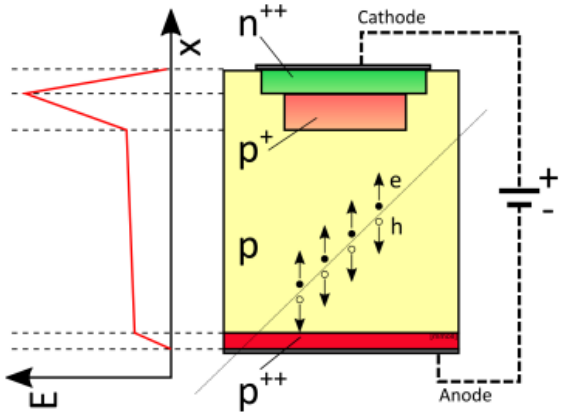

High energy particles (n, p⁺, e⁻ …) → *Si (LGAD)* → E_K>25 eV → Vacancy + Interstitial → *point defects (V-O, C-O, ..)*

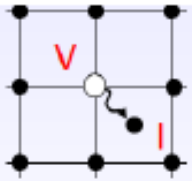

Si (LGAD) → E_K > 5 keV → *point defects and clusters of defects*

⟹ *radiation induced degradation of the highly boron-doped gain-layer*

⟹ *decrease of the signal gain with increasing particle fluence*

*„boron deactivation“ ⟹ ACCEPTOR REMOVAL EFFECT by **BiOi** formation*

Boron-removal IR vs. initial boron concentration

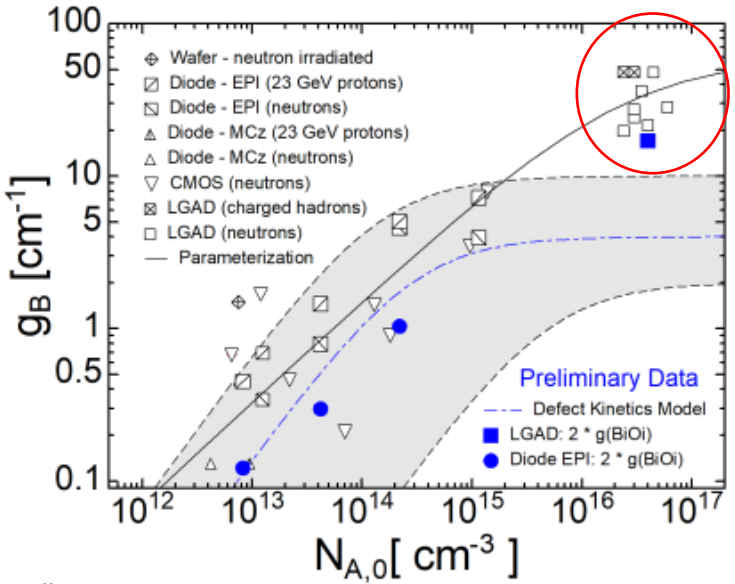

Moll, PoS 2019 VERTEX

defect kinetics model *(almost all intersitials go into BiOi or CiOi)*

for LGADs: generation rates that reflect the observed AR (deactivation of boron) cannot be explained by the interstitial related defect concentrations observed in highly B-doped Si

Torino Parametrization: Ferrero et al. NIMA 919 (2019) 16-26

Motivation

Moll, PoS 2019 VERTEX

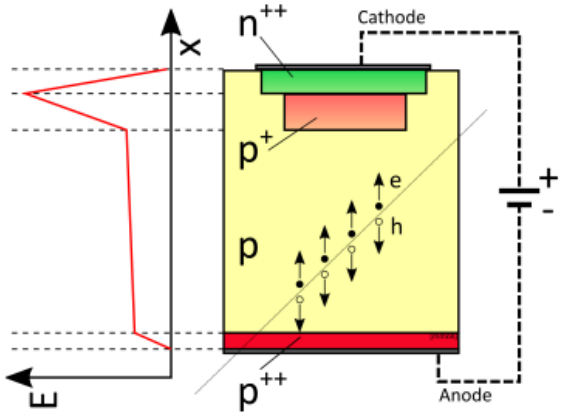

High energy particles (n, p⁺, e⁻ …) → *Si (LGAD)* → E_K>25 eV → Vacancy + Interstitial → *point defects (V-O, C-O, ..)*

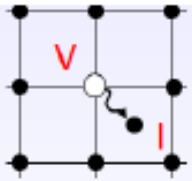

Si (LGAD) → E_K > 5 keV → *point defects and clusters of defects*

⟹ *radiation induced degradation of the highly boron-doped gain-layer*
⟹ *decrease of the signal gain with increasing particle fluence*

*„boron deactivation“ ⟹ ACCEPTOR REMOVAL EFFECT by **BiOi** formation*

Boron-removal IR vs. initial boron concentration

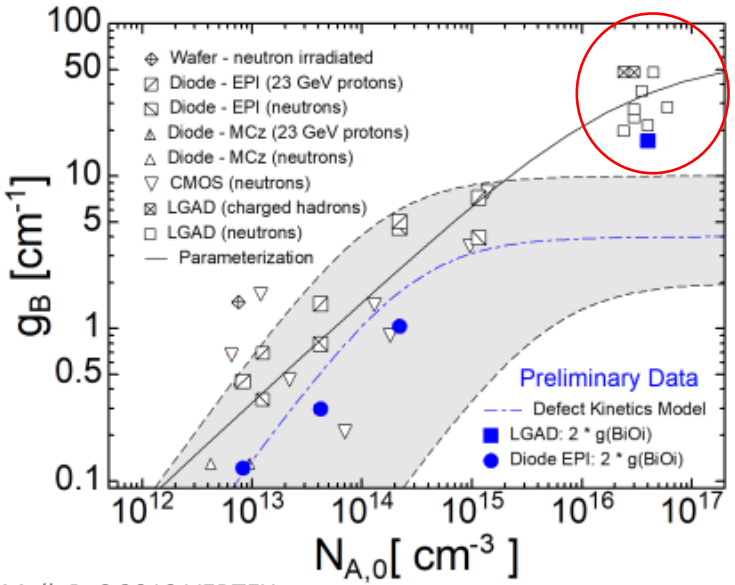

Moll, PoS 2019 VERTEX

defect kinetics model *(almost all intersitials go into BiOi or CiOi)*

Torino Parametrization: Ferrero et al. NIMA 919 (2019) 16-26

for LGADs: generation rates that reflect the observed AR (deactivation of boron) cannot be explained by the interstitial related defect concentrations observed in highly B-doped Si

What other defect formation mechanism lead to the deactivation of acceptors?

Can we get information about gain-layer defects by using defect spectroscopy methodes like DLTS or TSC?

DLTS & TSC

DLTS: Deep Level Transient Spectroscopy

(1) Junction under reverse bias @ different temperatures→ defect states unoccupied
(2) Injection pulse (electrical or optical) → injection of minority and/or majority carriers → occupation of defect levels
(3) Junction under reverse bias → charge carriers thermally emitted → change in capacitance

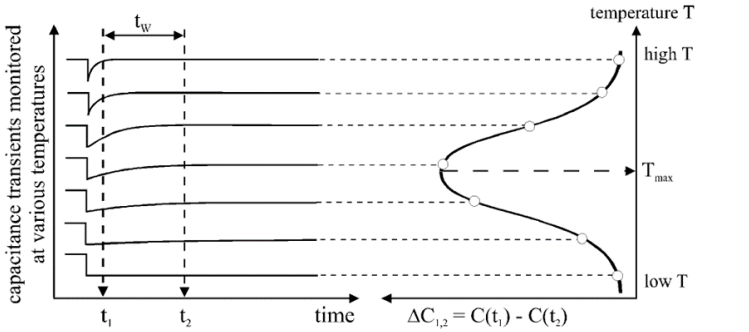

Moll thesis 1999

Defect parameters:
activation energy
capture cross section
defect concentrations

DLTS limited to defect concentrations
$N_t \approx 0.1\text{-}0.3 * N_{doping}$

TSC: Thermally Stimulated Current

(1) Junction under reverse bias during cooling down of the sample to T_{Fill}
→ defect states unoccupied
(2) Injection pulse (electrical or optical) → injection of minority and/or majority carriers
→ occupation of defect levels
(3) Junction under reverse bias & temperature raised
→ monitoring the discharging current due to thermal emission from the defect levels

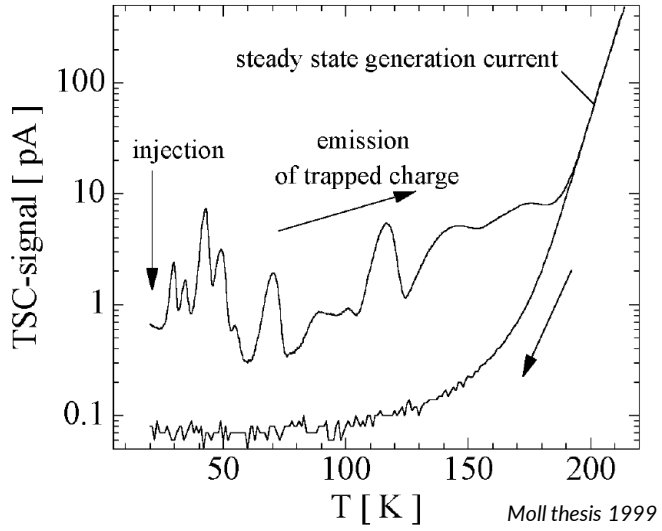

Moll thesis 1999

LGADs & PiNs neutron irradiated

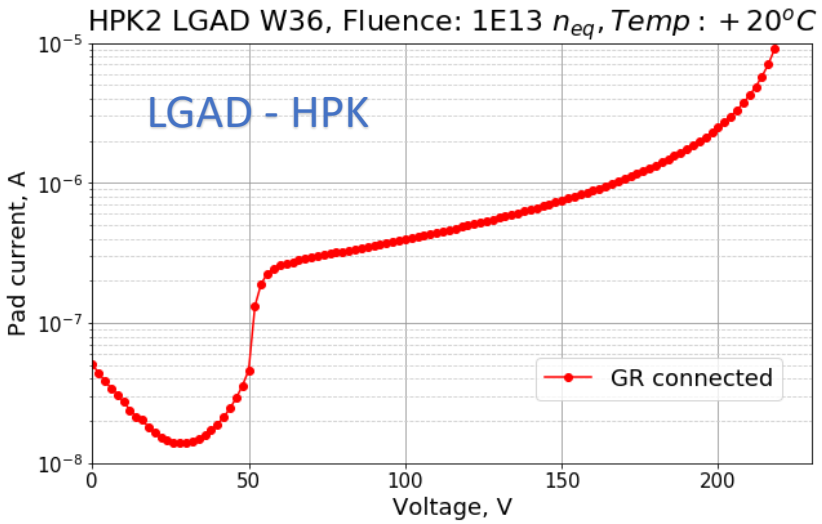

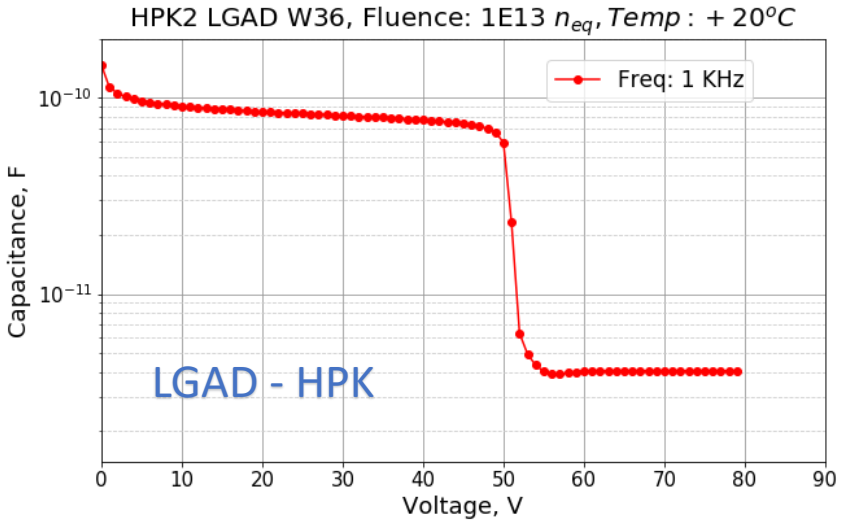

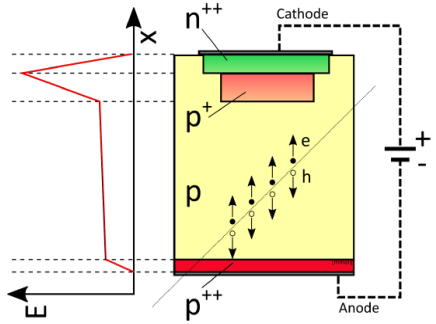

	fluence (neq/cm²)	U_{depl} (V)
LGAD - HPK W36 S3 – L15P5	1E+13	~ 50
PiN – HPK W42 S4 – L14P5	1E+13	~ 5

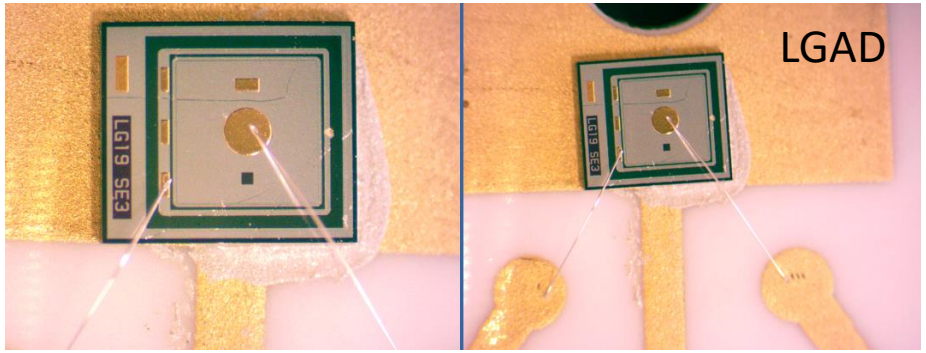

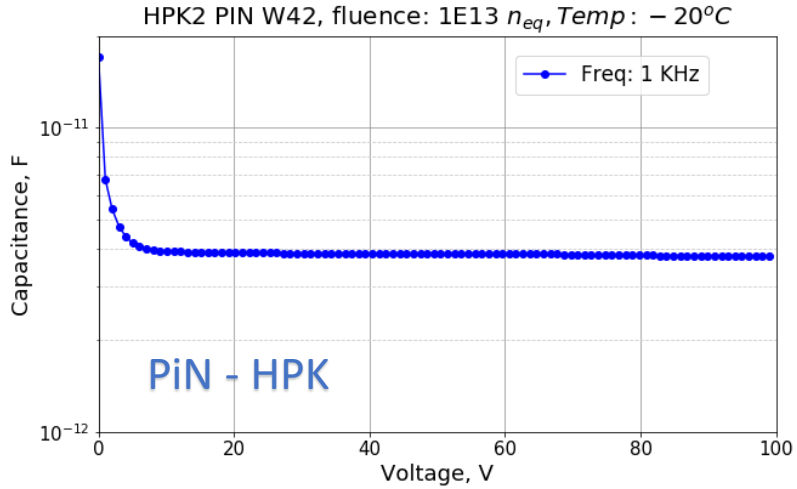

LGADs & PiNs neutron irradiated

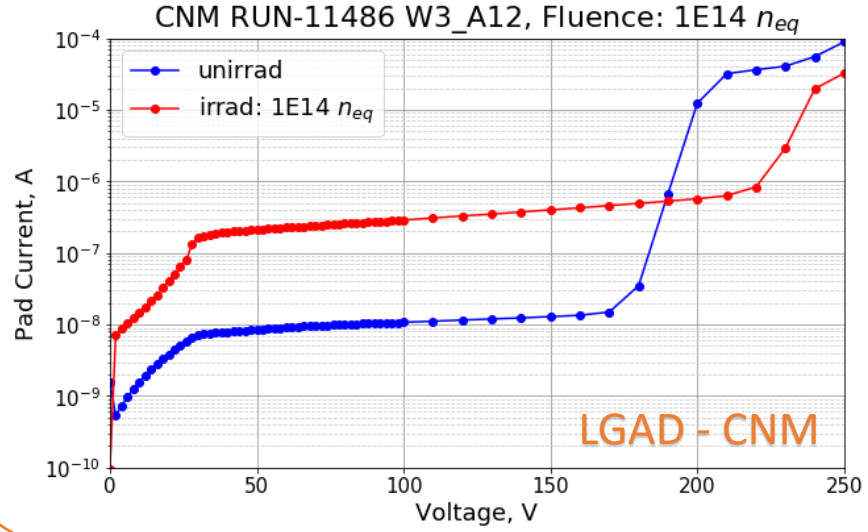

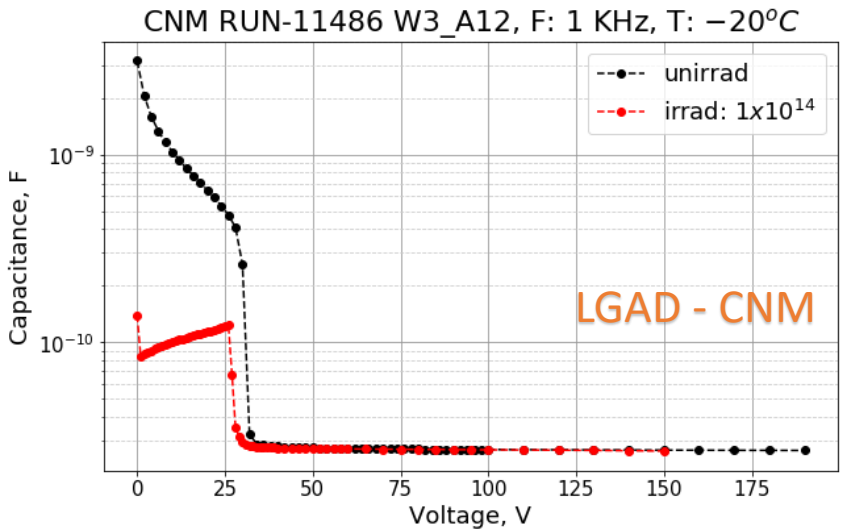

	fluence (neq/cm²)	U_{depl} (V)
LGAD - HPK W36 S3 – L15P5	1E+13	~ 50
PiN – HPK W42 S4 – L14P5	1E+13	~ 5
LGAD – CNM W2 – U23	1E+14	~ 30
LGAD – CNM W3 – A12	1E+14	~ 30
PiN – CNM W2 – X22	1E+14	~ 2
LGAD – CNM W2 – W22	1E+15	

SOI –wafer *(run11486) – (351 µm thick):*
p-type active layer
(B-doped, resistivity > 5000 Ωcm, 50 µm)
oxide layer (1 µm)
p-type support-wafer (B-doped, 300 µm, low resistivity)

wafer differ in gain layer:
= W2: medium dose / higher energy
= W3: high dose / low energy

LGADs & PiNs neutron irradiated

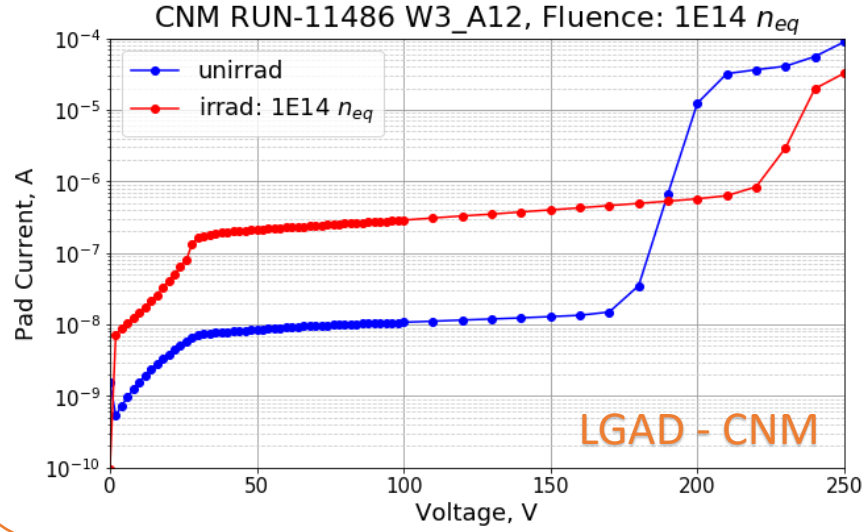

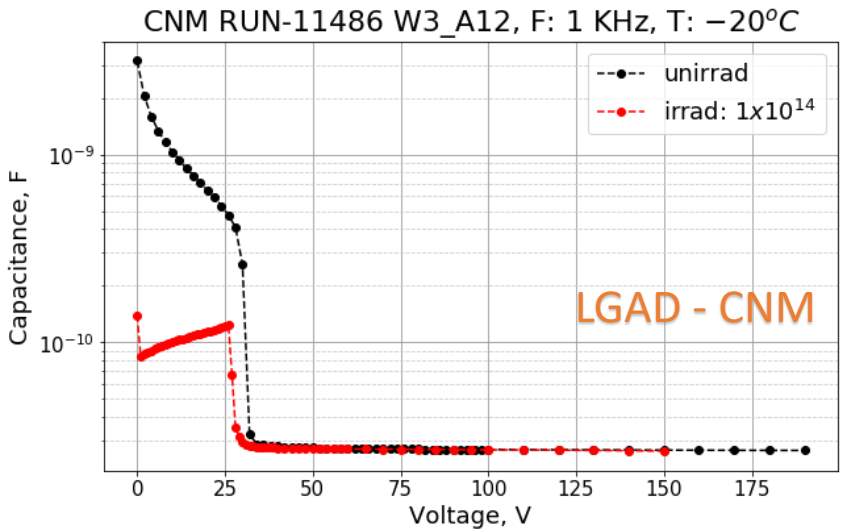

	fluence (neq/cm²)	U_{depl} (V)
LGAD - HPK W36 S3 – L15P5	1E+13	~ 50
PiN – HPK W42 S4 – L14P5	1E+13	~ 5
LGAD – CNM W2 – U23	1E+14	~ 30
LGAD – CNM W3 – A12	1E+14	~ 30
PiN – CNM W2 – X22	1E+14	~ 2
LGAD – CNM W2 – W22	1E+15	

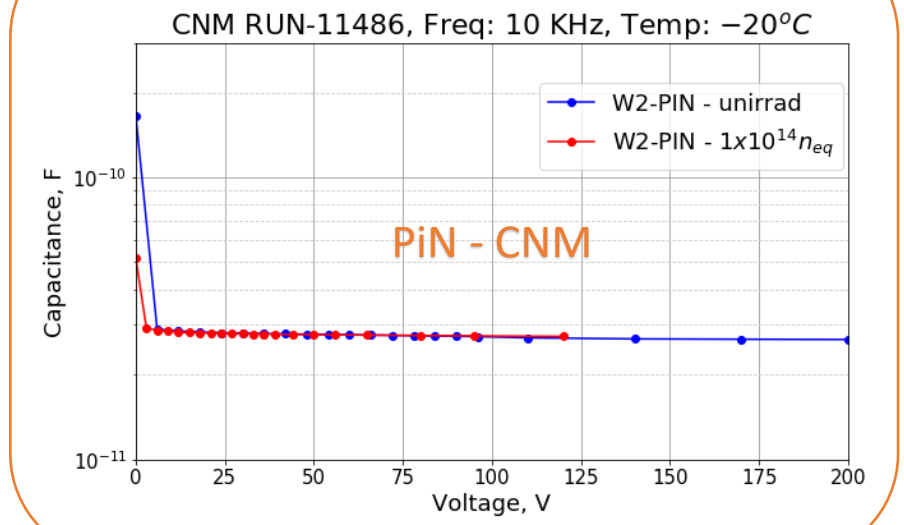

LGADs & PiNs neutron irradiated

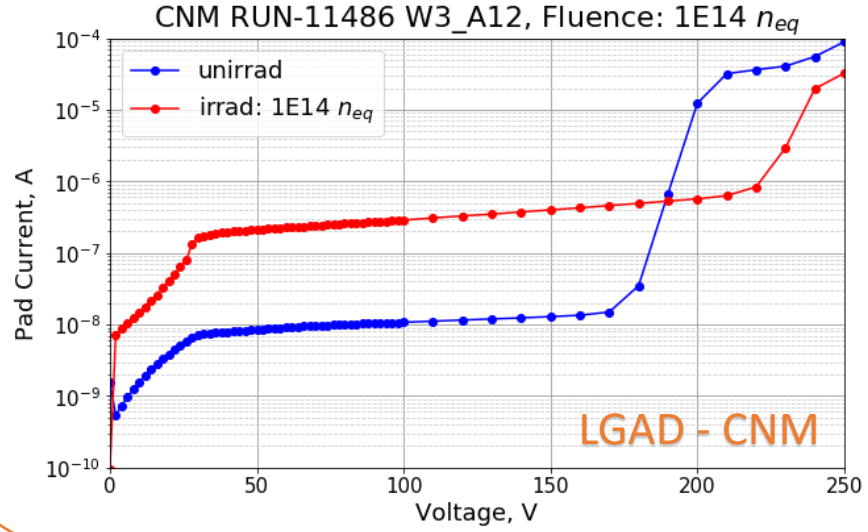

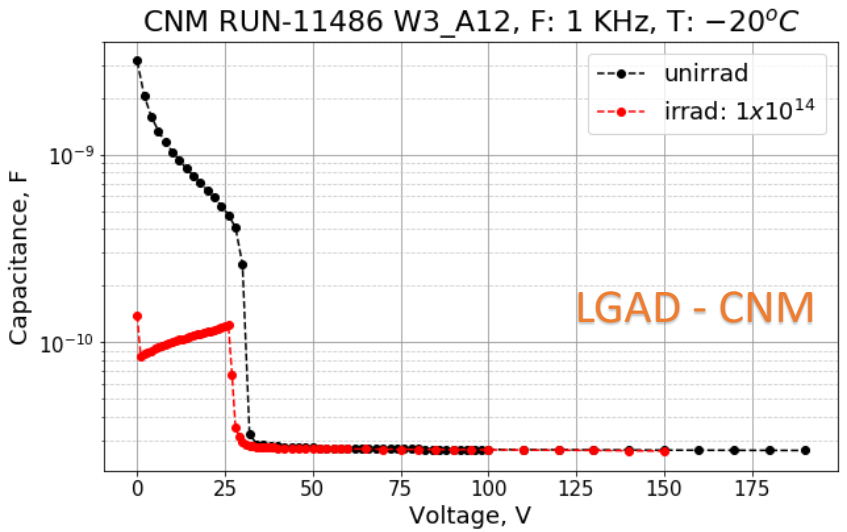

	fluence (neq/cm²)	U_{depl} (V)
LGAD - HPK W36 S3 – L15P5	1E+13	~ 50
PiN – HPK W42 S4 – L14P5	1E+13	~ 5
LGAD – CNM W2 – U23	1E+14	~ 30
LGAD – CNM W3 – A12	1E+14	~ 30
PiN – CNM W2 – X22	1E+14	~ 2
LGAD – CNM W2 – W22	1E+15	

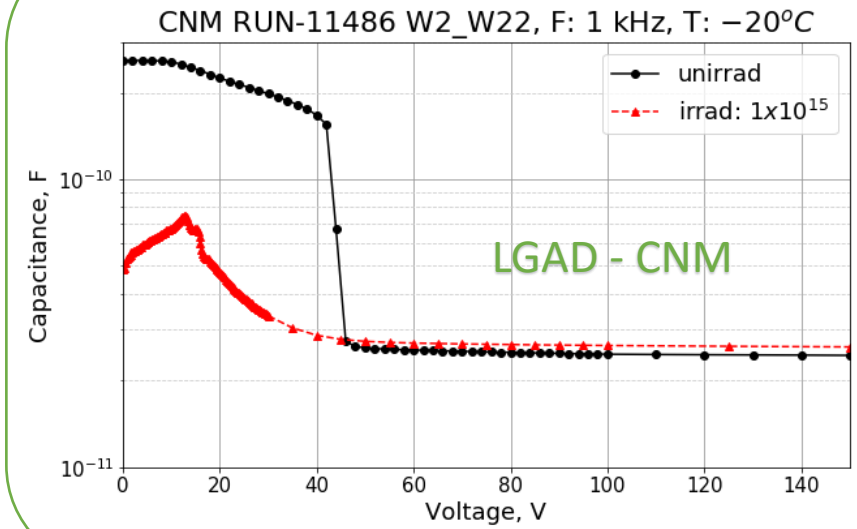

Frequency dependence

LGAD – HPK (1E+13 neq/cm²)

unirradiated

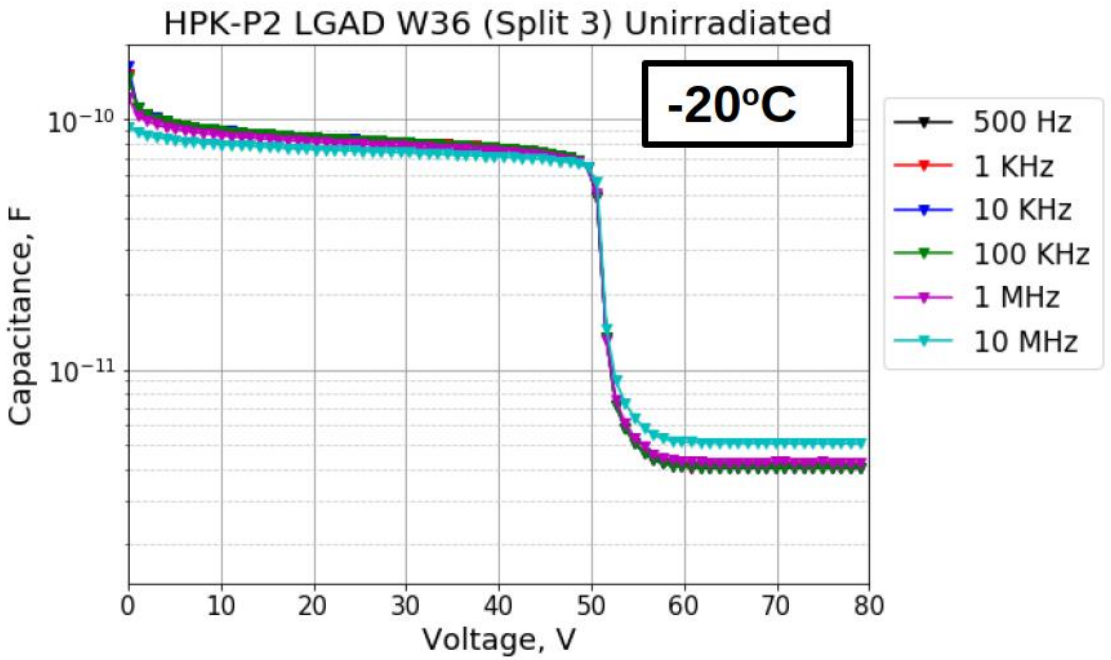

irradiated

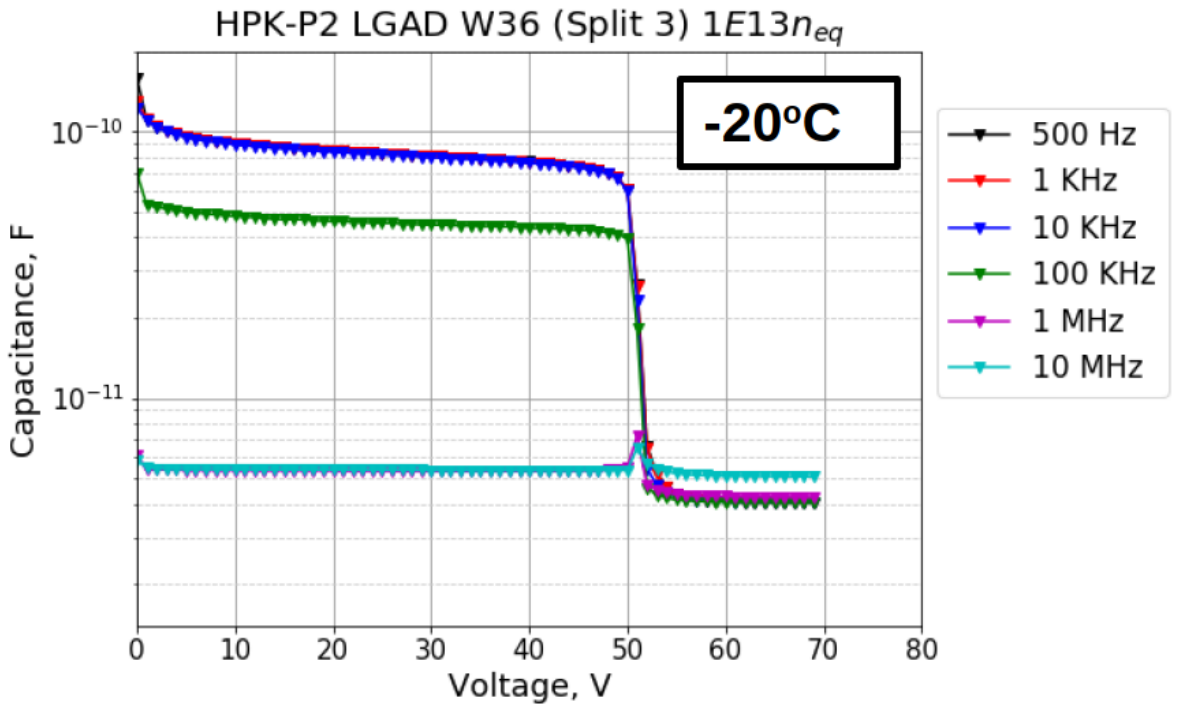

after irradiation: capacitance drops at higher measurement frequencies

Frequency dependence & temperature dependence

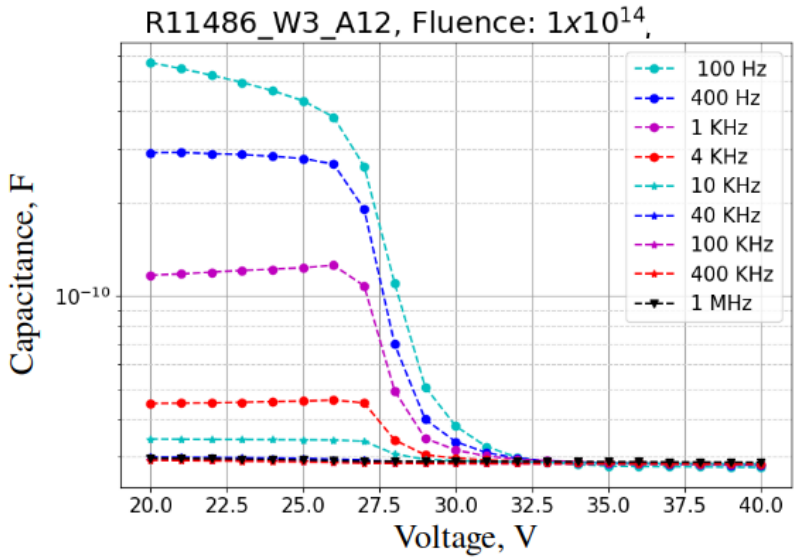

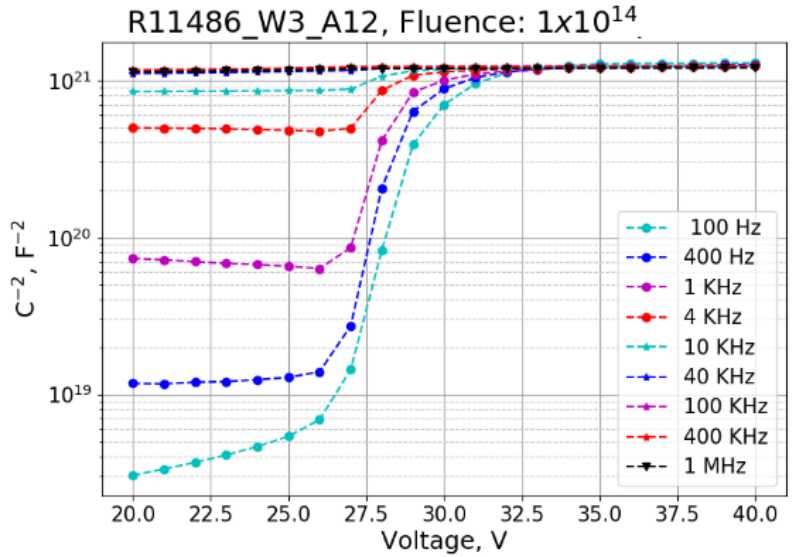

LGAD – CNM (1E+14 neq/cm²)

↑F → ↓C

↓T → ↓C

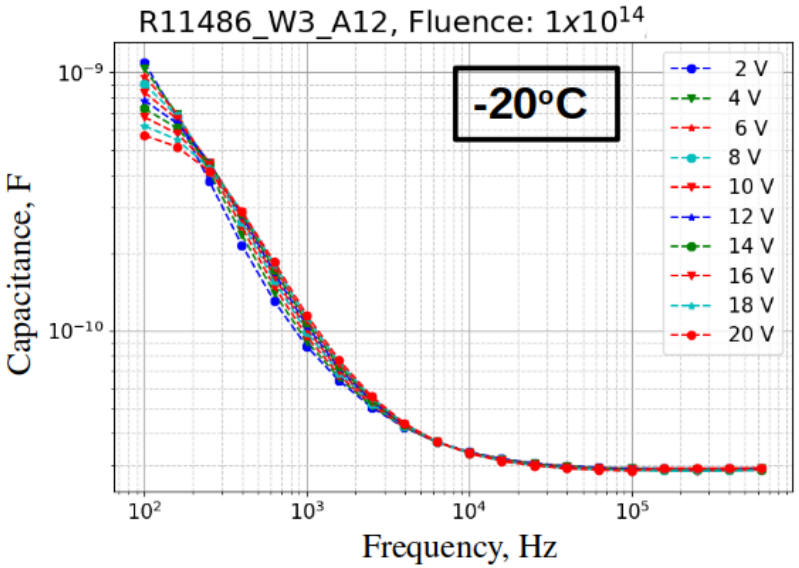

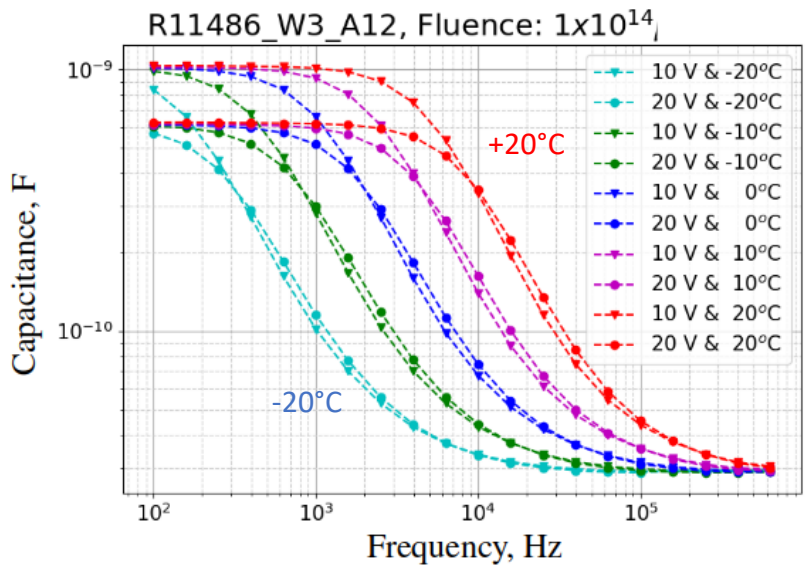

Frequency dependence & temperature dependence

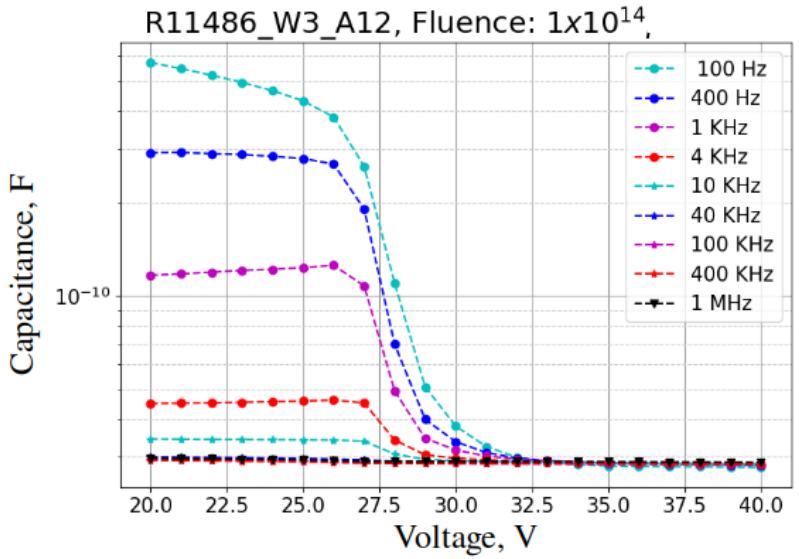

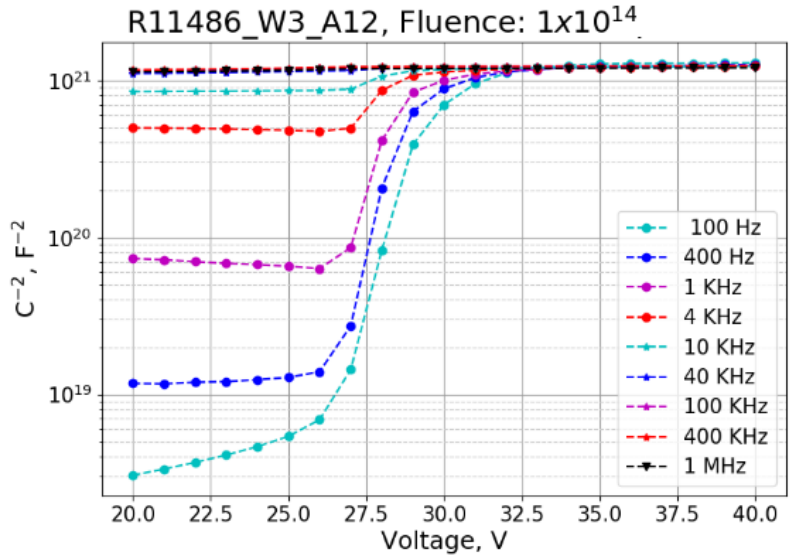

LGAD – CNM (1E+14 neq/cm²)

↑F → ↓C

↓T → ↓C

DLTS defect characterization: performed at low T (> 20K) and high frequency (1MHz)

Capacitance in the GL drops to the bulk value

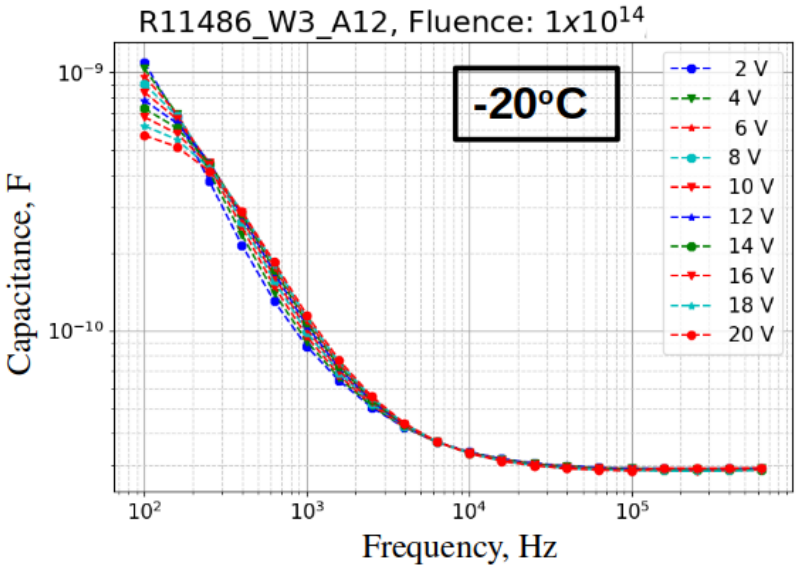

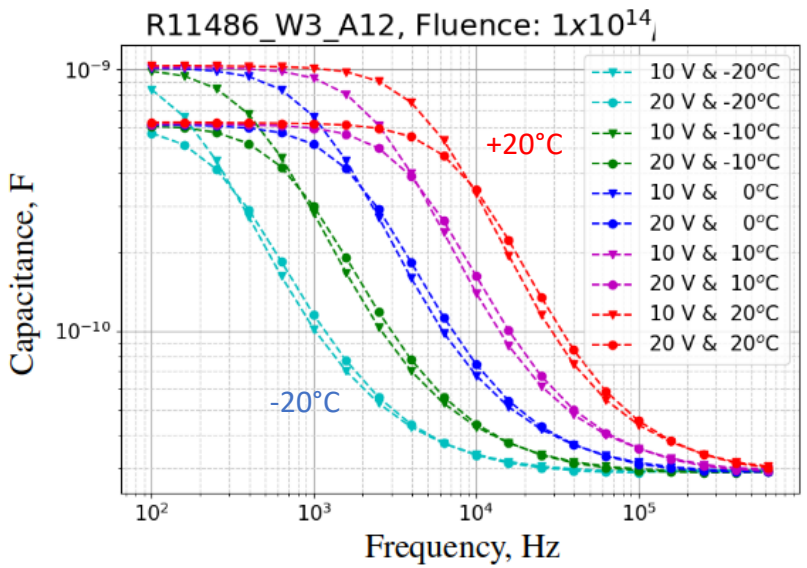

DLTS on LGADs

Majority & minority carrier injection

peak I:
E_t-E_c ~ 0.27 eV
sigma ~ 10^{-17} cm²

peak II(a):
E_t-E_c ~ 0.3 – 0.33 eV
sigma ~ 10^{-16} cm²

peak III:
E_t-E_c ~ 0.72 eV
sigma ~ 10^{-8} – 10^{-11}cm²

LGADs

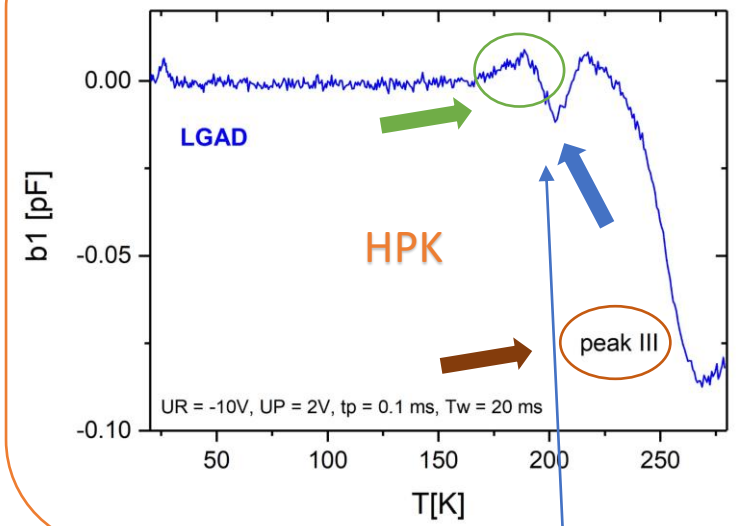

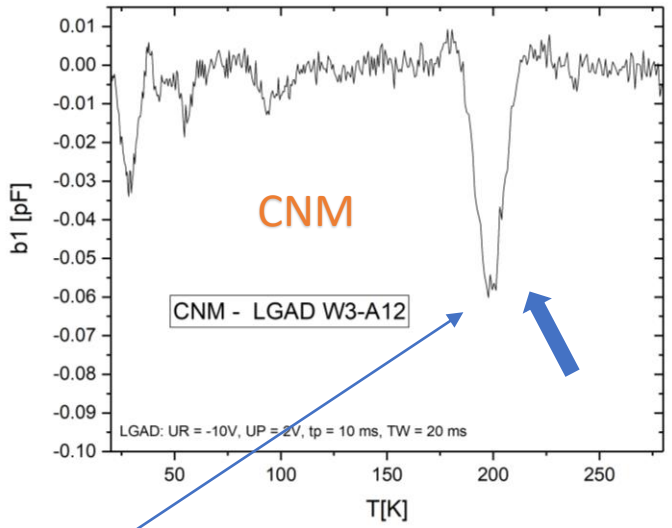

E_t-E_c ~ 0.35 eV
sigma ~ 10^{-16} cm²

HPK-PiN (1E+13 neq/cm²)

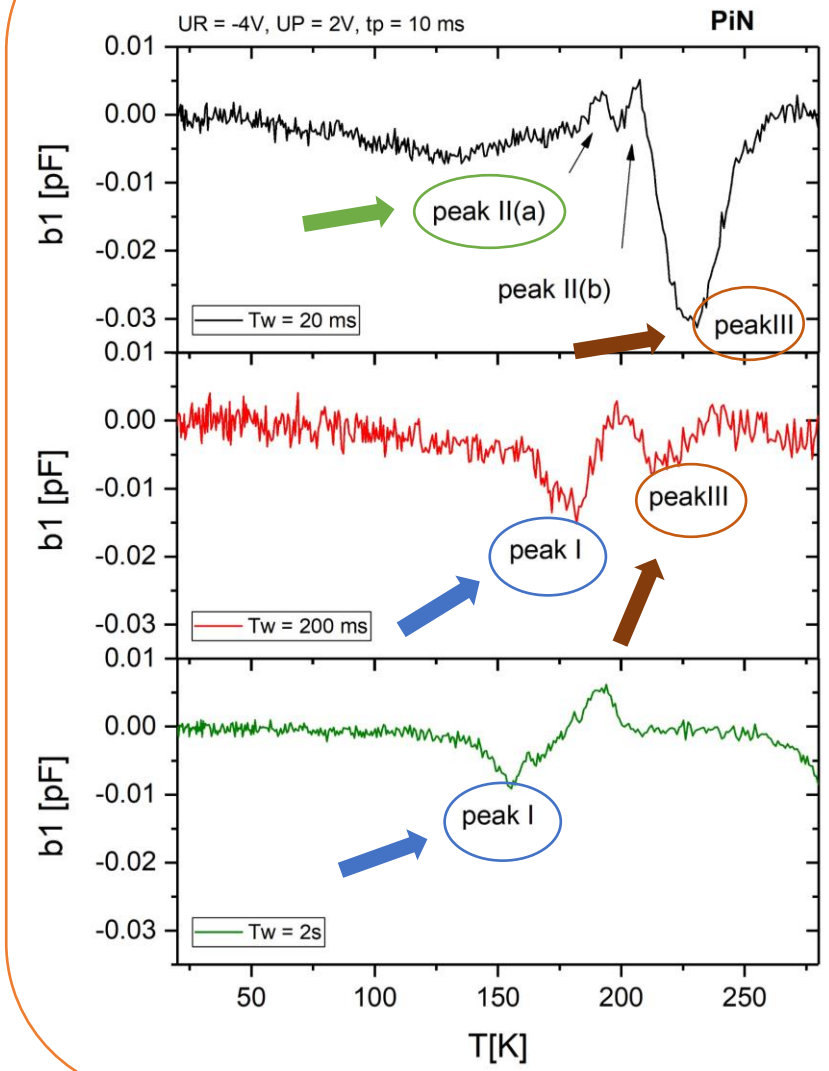

DLTS on LGADs

Majority & minority carrier injection

⟹ Detection of a whole set of defects possible
⟹ How trustable due to the **capacitance drop**?
⟹ Defect concentrations not possible to evaluate
⟹ BiOi of the gain-layer not possible to detect

E_t-E_c ~ 0.25 eV
sigma ~ 10^{-15}cm²

LGADs

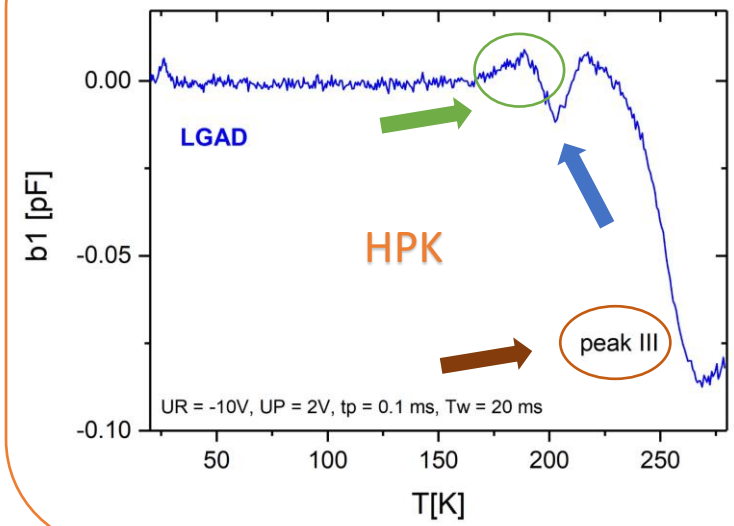

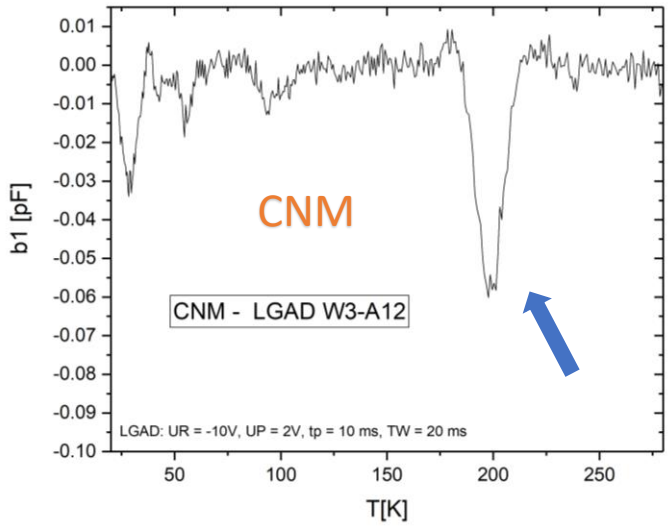

HPK-PiN (1E+13 neq/cm²)

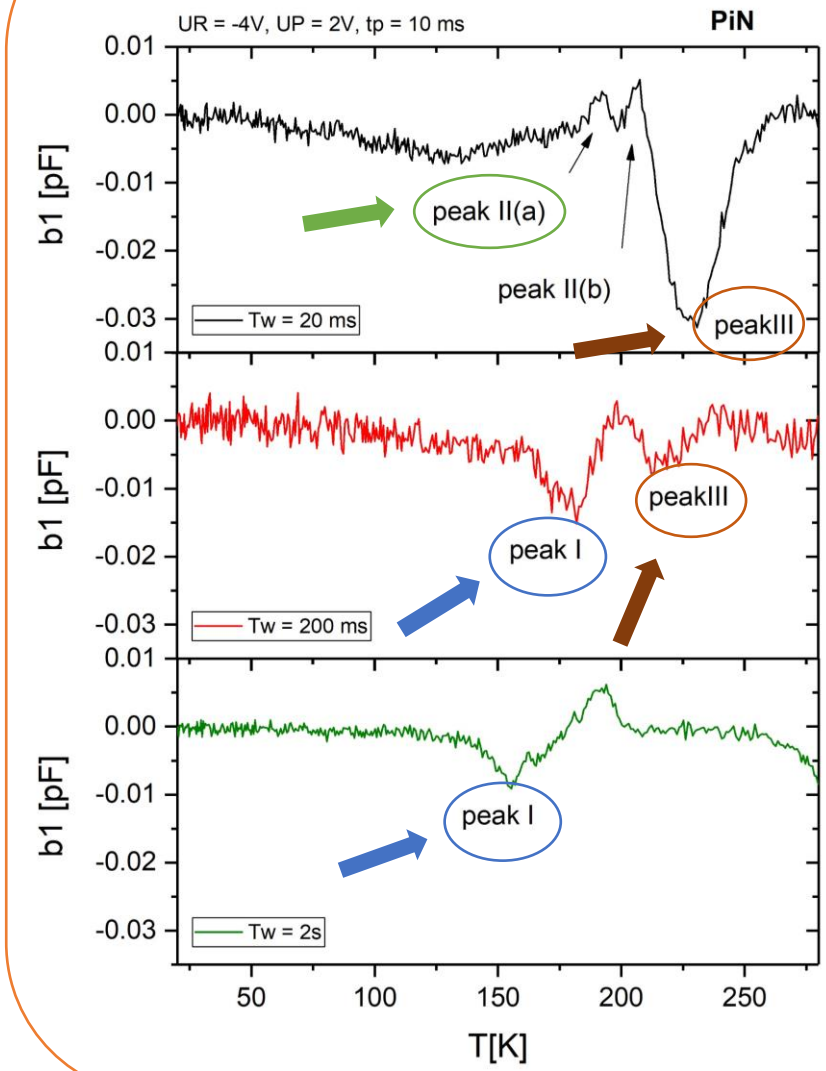

TSC on PiNs

$$n_{t,0} = 2\frac{Q_t}{q_0 A W}$$

HPK-PiN (1E+13 neq/cm²)

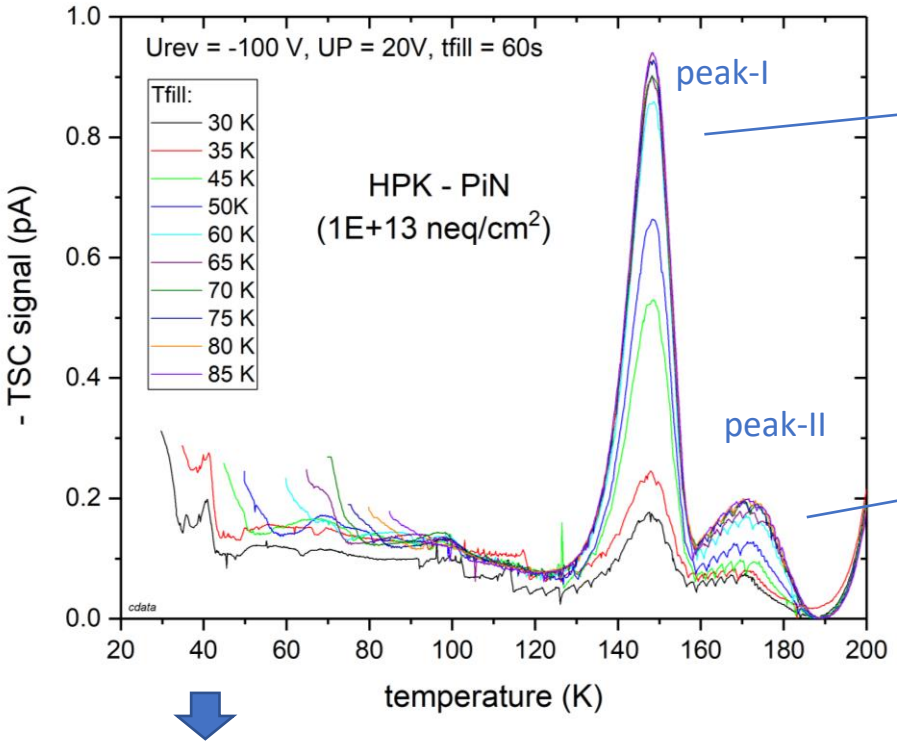

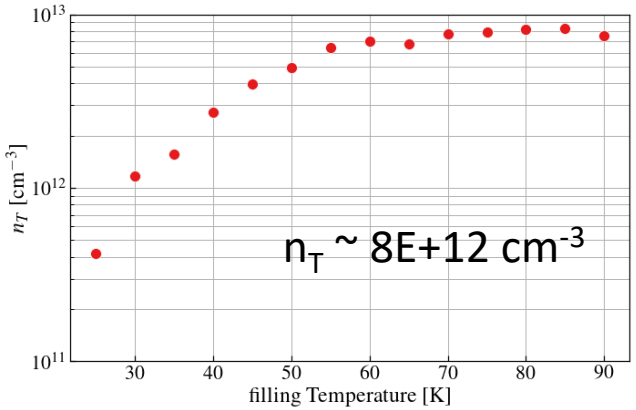

n_T ~ 8E+12 cm^{-3}

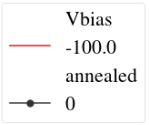

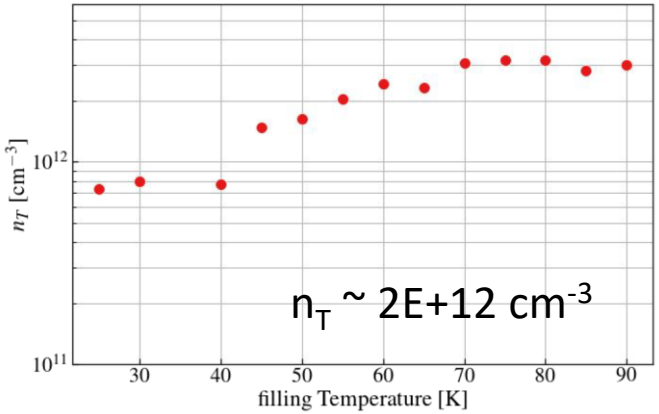

n_T ~ 2E+12 cm^{-3}

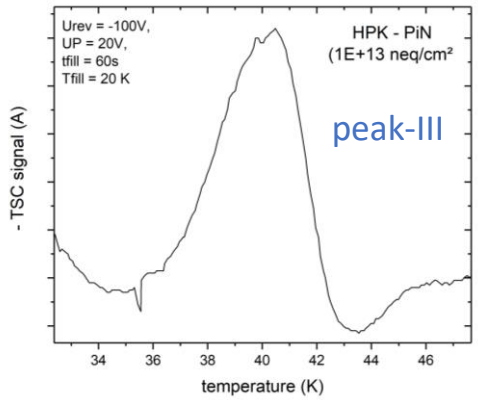

n_T ~ 4E+11 cm^{-3}

Fitting & Simulation:

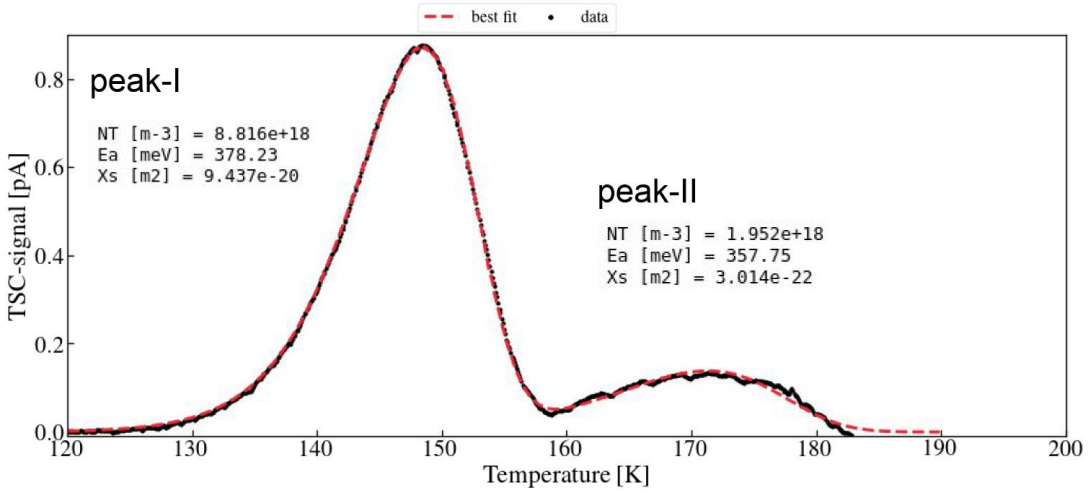

TSC on PiNs

CNM-PiN (1E+14 neq/cm²)

Bias dependence

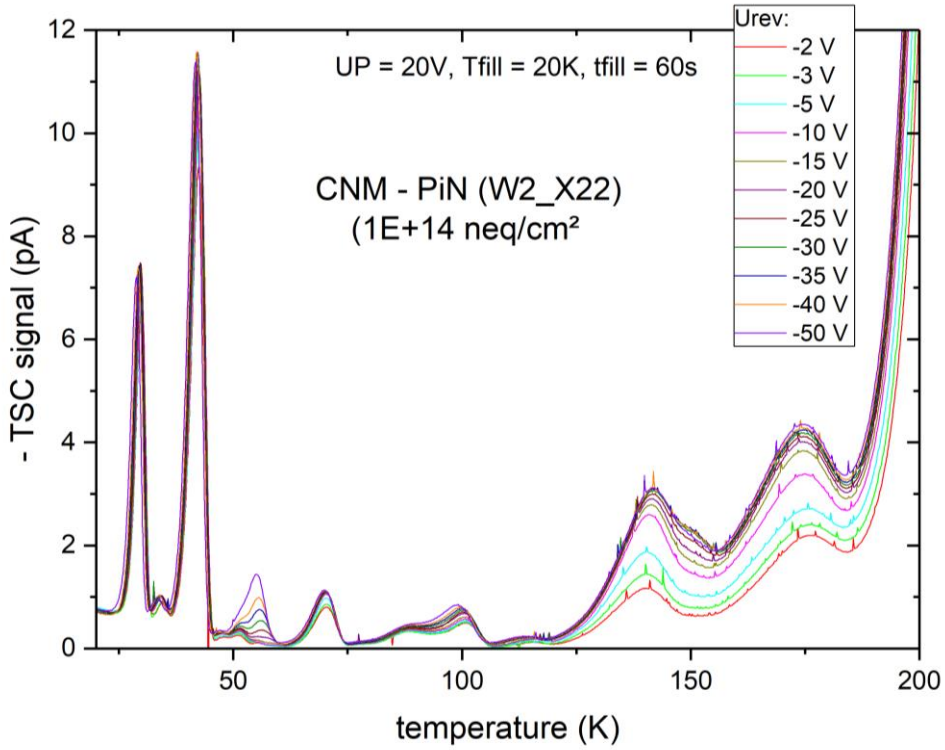

Filling-temperature dependence

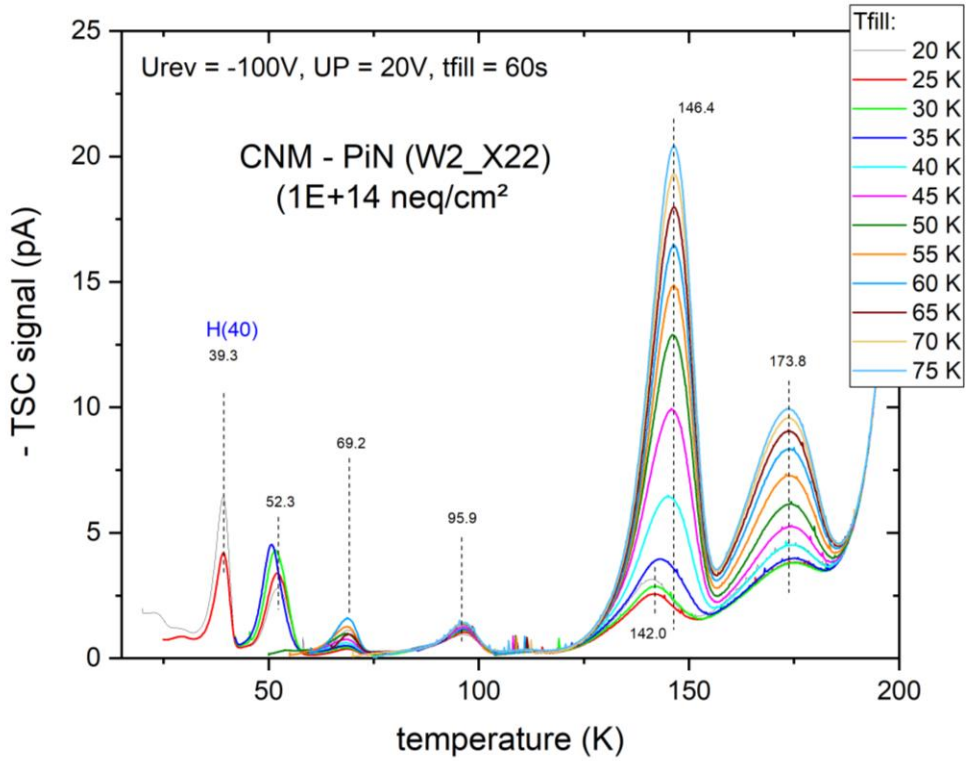

TSC on LGADs

HPK – 1E+13 neq/cm²

Variation of the depletion voltage ($U_{depl-GL}$ ~ -50V)

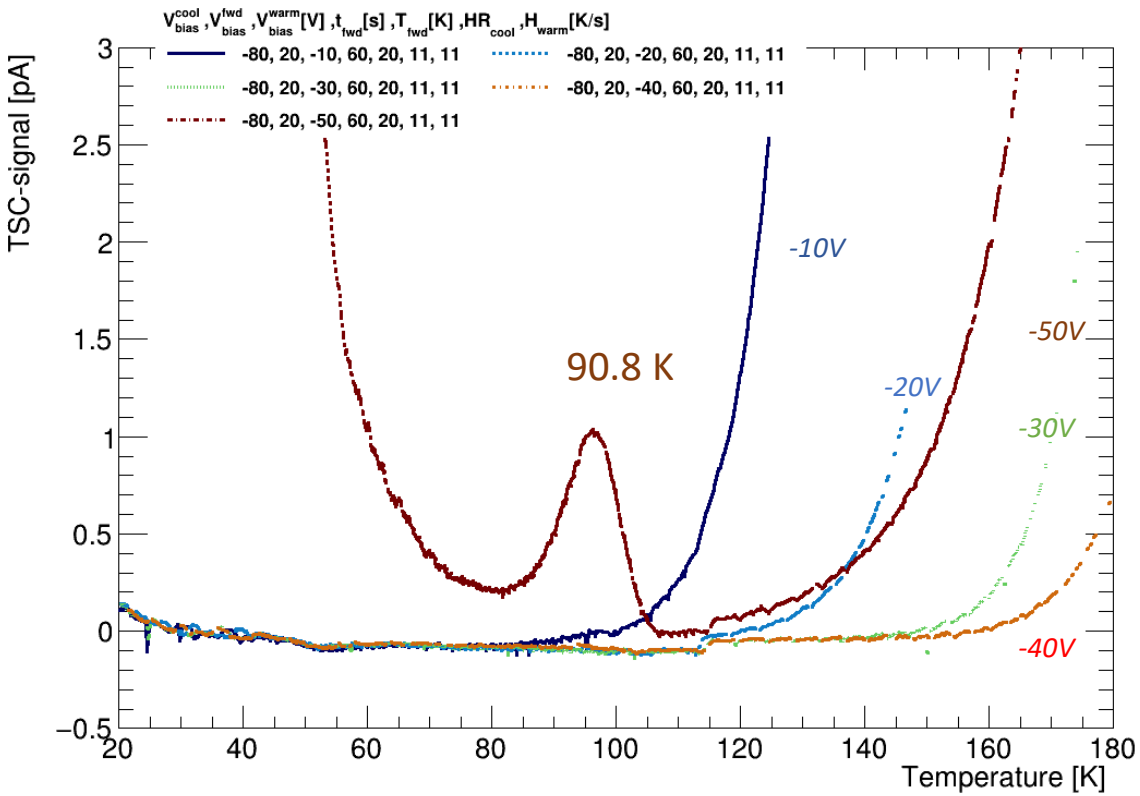

if voltage > $U_{depl-GL}$: defect level detected @ 90.8 K

TSC on LGADs

HPK – 1E+13 neq/cm²

Variation of the depletion voltage ($U_{depl-GL}$ ~ -50V)

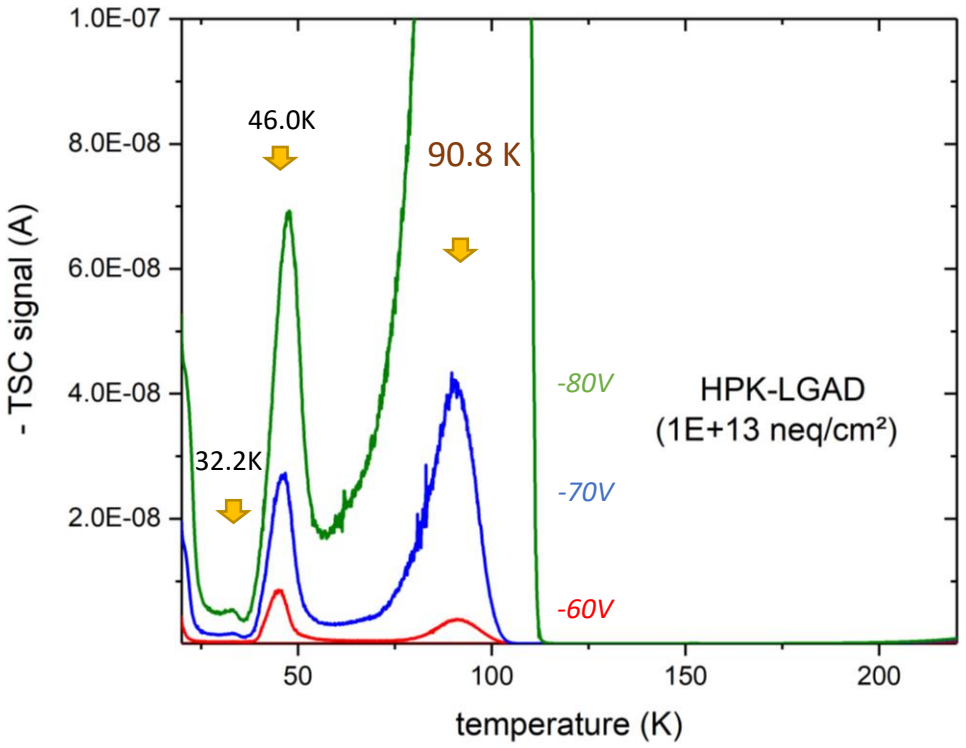

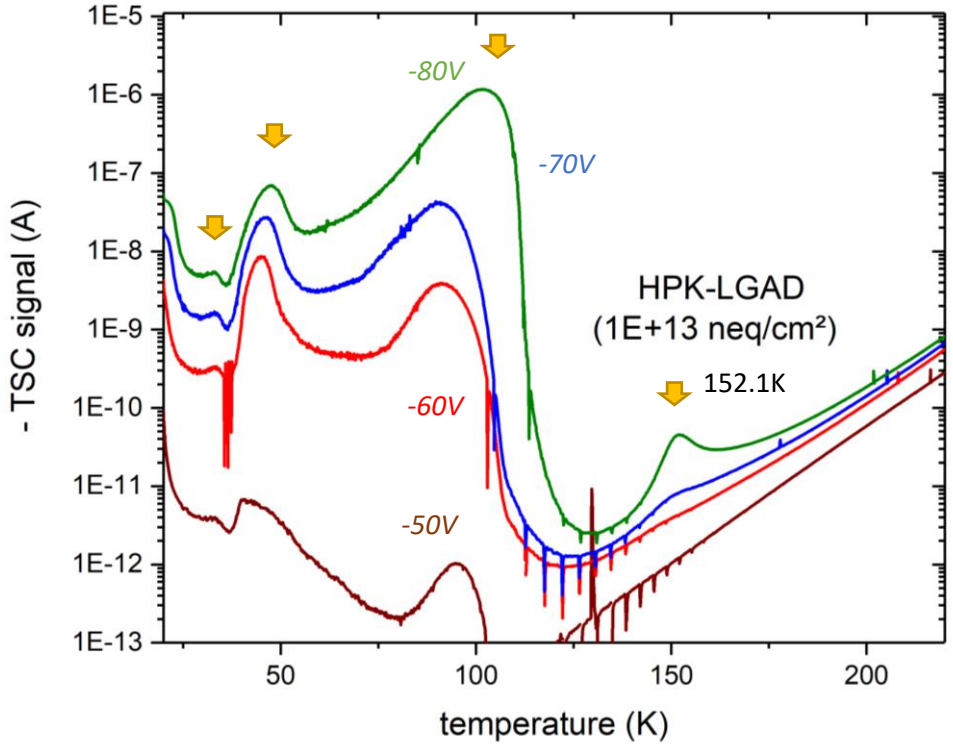

⇒ *Defect level intensity strongly increases with increasing bias*

… charge multiplication effect due to the gain

… carrier concentration determination difficult

TSC on LGADs

CNM – 1E+14 neq/cm²

Variation of the depletion voltage ($U_{depl-GL}$ ~ -30V)

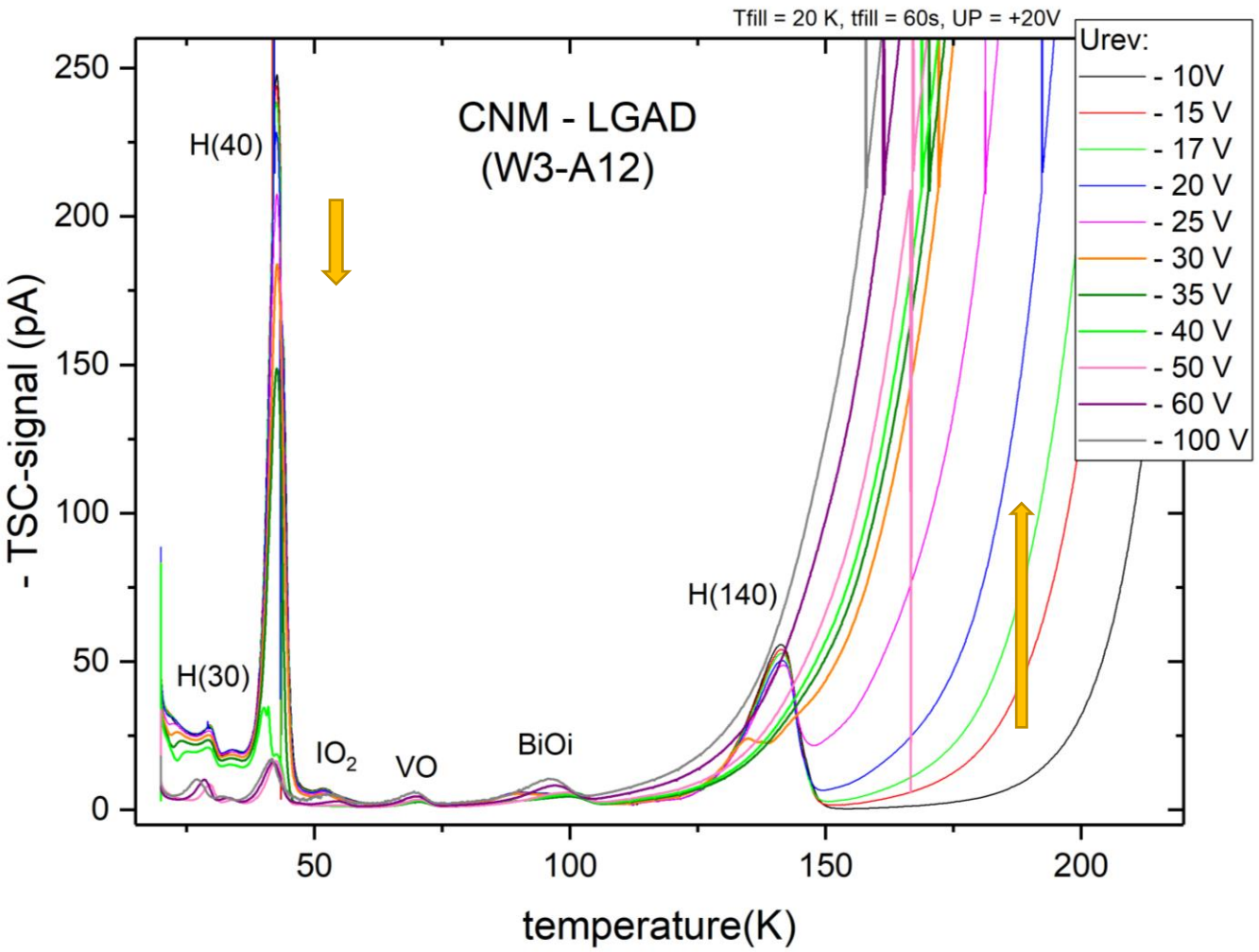

higher irradiation ⟹ more defect levels detected (even if $U_{rev} < U_{depl-GL}$)

Defect level intensity depends on the reverse bias applied
⟹ peaks at low T: higher intensity if $U_{rev} < U_{depl-GL}$

less pronounced charge multiplication effect compared to the lower irradiated HPK-LGADs (especially at low T)

at higher T: leakage current amplification remarquely increase with the applied voltage
⟹ overlapp the current signal fom defects

TSC on LGADs

CNM – 1E+14 neq/cm²

Variation of the depletion voltage ($U_{depl\text{-}GL}$ ~ -30V)

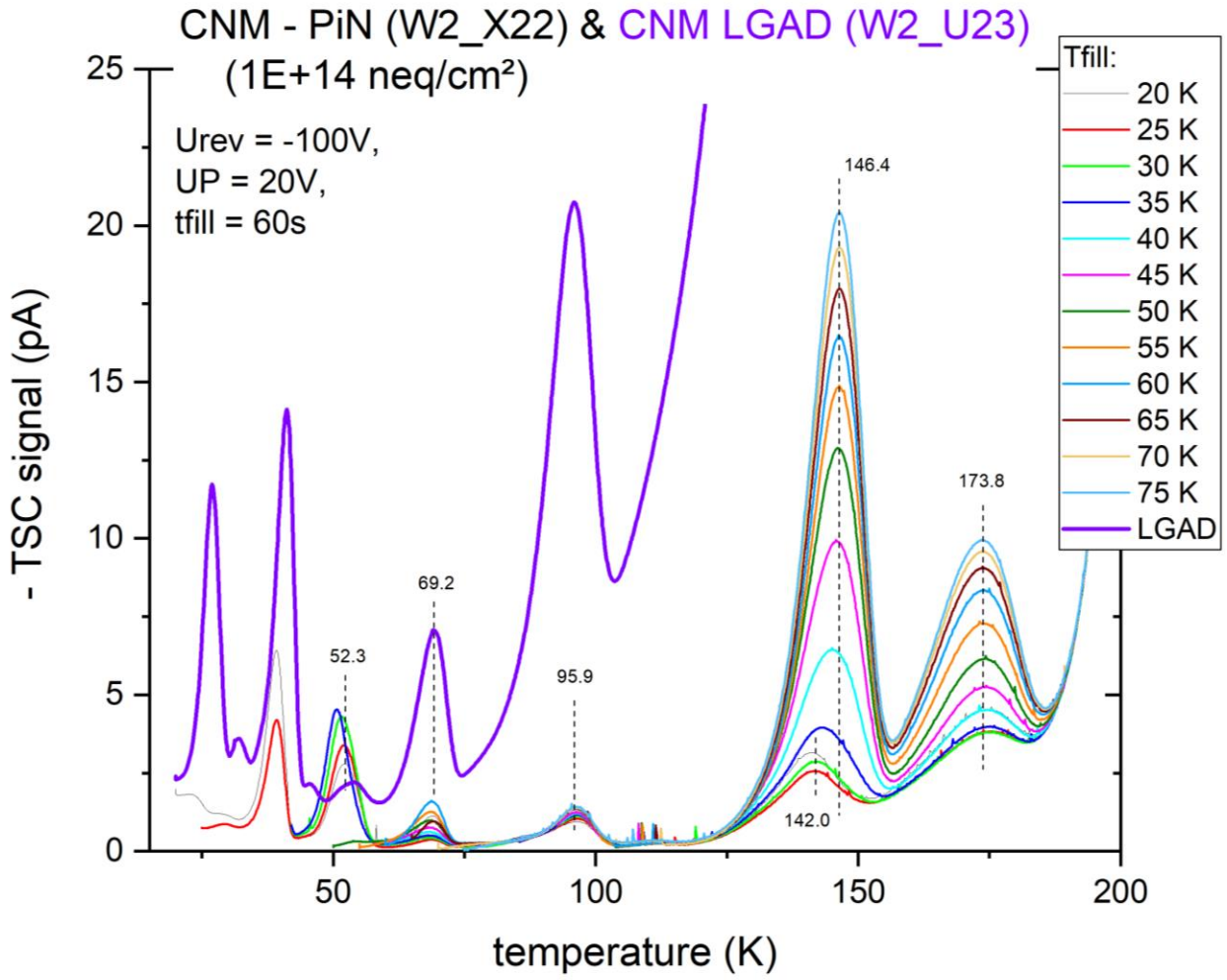

charge multiplication effect of the LGAD

TSC on LGADs

CNM – 1E+14 neq/cm²

Variation of the depletion voltage ($U_{depl-GL}$ ~ -30V)

+ implementing a high voltage step after the filling pulse

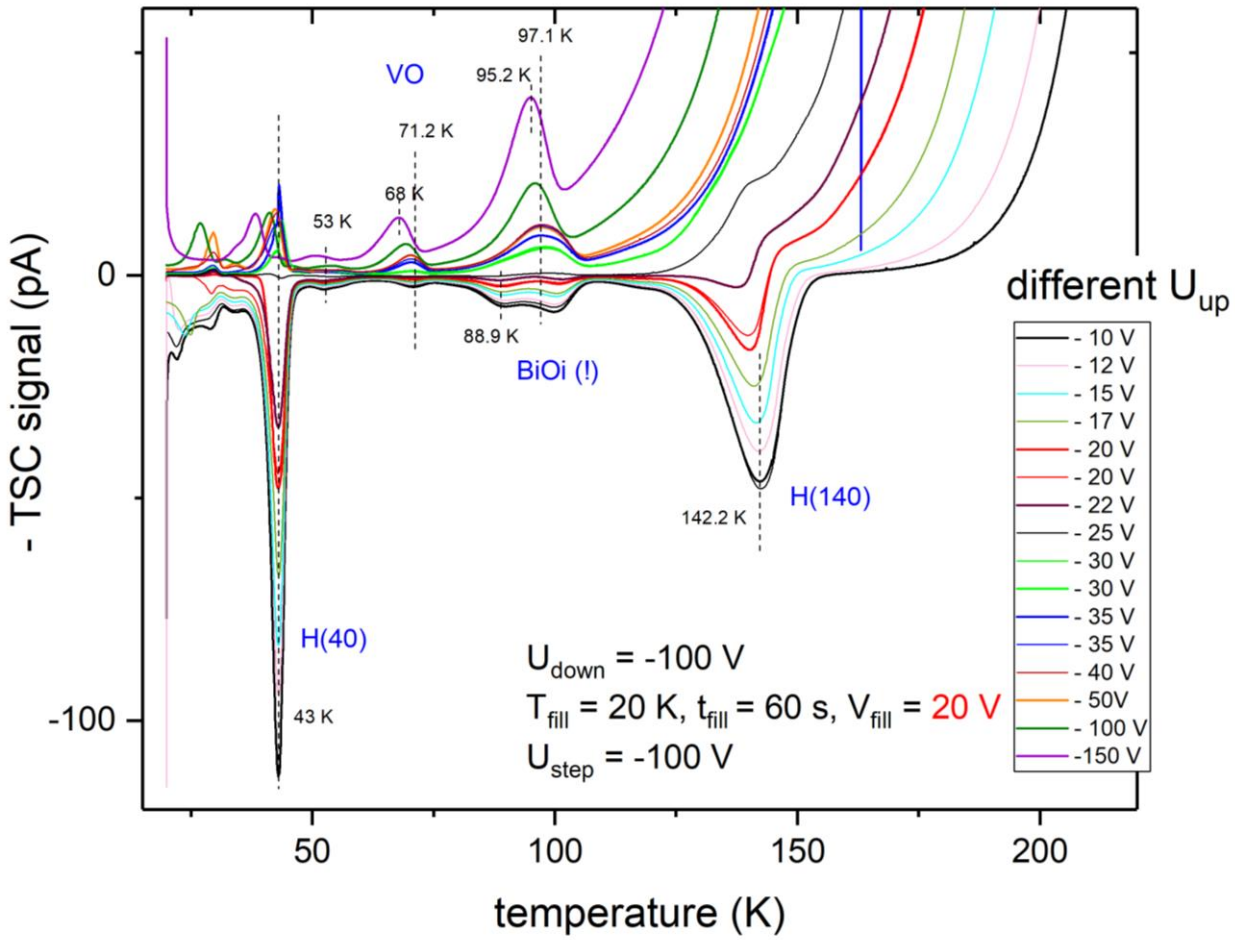

TSC measurement cycle:

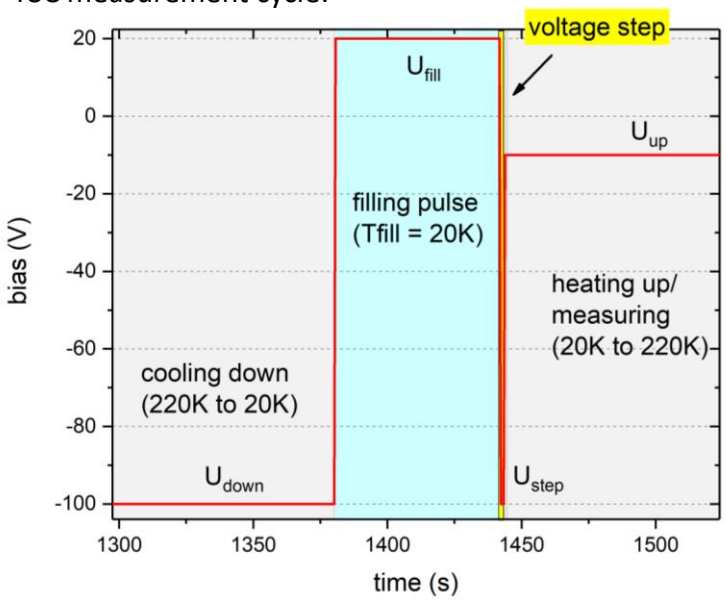

Sign change of the TSC signal at U_{up} about - 25 V ($U_{depl-GL}$ ~ -30V)

TSC on LGADs

HPK – 1E+13 neq/cm²

Variation of the depletion voltage ($U_{depl-GL}$ ~ -50V)

+ implementing a high voltage step after the filling pulse

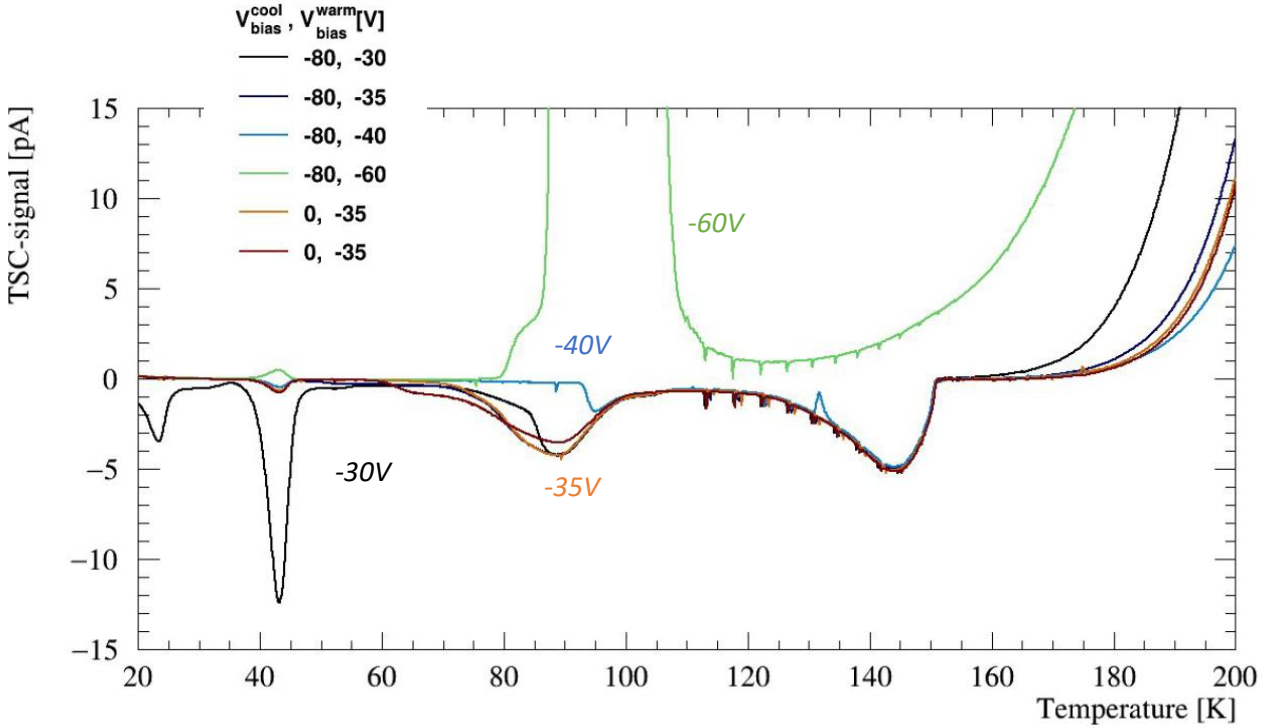

TSC measurement cycle:

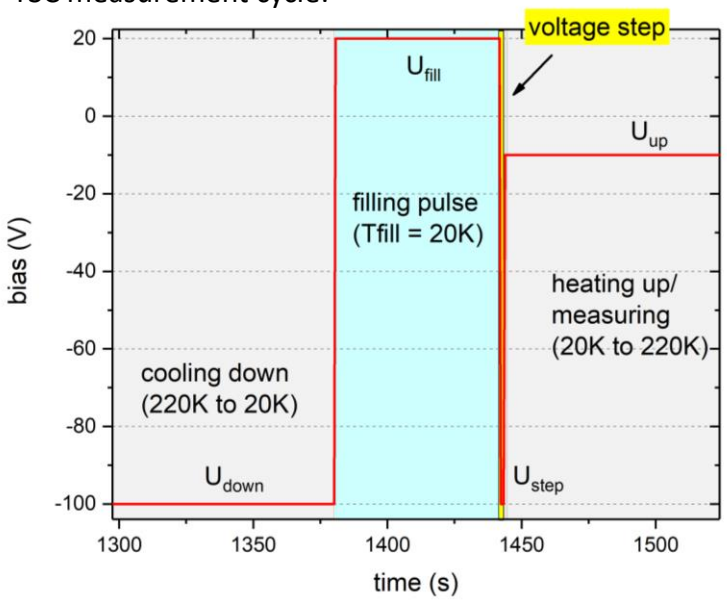

Sign change of the TSC signal at ca. - 50 V ($U_{depl-GL}$ ~ -50V)

⟹ *internal electrical polarization fields that induce an inverse current signal*

Summary

- DLTS & TSC characterization of HPK & CNM LGADs & PiNs irradiated with neutrons (1E+13 – 1E+15 neq/cm²)
- **DLTS** studies restricted by the capacitance drop observed after irradiation
- **TSC:** Detection of a variety of defect states possible
  ⟹ higher irradiation: more defects & less gain
  ⟹ assignment of defect levels to the gain- or bulk-area is challenging, but ongoing

  pronounced charge multiplication effect & leakage current amplification
  - effect increases with higher radiation & higher T
  - overlapp defect emission currents
  - restrict defect determination & defect concentration determinations
- Reverse internal fields possible to „activate“ - influence the sign of the TSC current signal

Outlook

*… using defect parameters from DLTS & TSC to **simulate TSC spectra + comparison of the PiN & LGAD data***
… ongoing identification of irradiation induced defects that degradate the device performance

… investigate highly irradiated, highly B-doped (1E+17 cm^{-3}) Si diodes: ….fabrication?

Thank you for your attention!